Pergamon

Int. J. Heat Mass Transfer. Vol. 38, No. 1, pp. 71–79, 1995

0017–9310/95 $9.50+0.00

0017–9310(94)00140–5

Exact solutions of Stefan problems for a heat front moving at constant velocity in a quasi-steady state

C. K. HSIEH

Mechanical Engineering Department, University of Florida, Gainesville, FL 32611, U.S.A.

(*Received* 13 *October* 1993 *and in final form* 25 *April* 1994)

Abstract—A source-and-sink method has been used to solve a Stefan problem imposed with a moving heat front travelling at constant velocity in a fixed direction. The problem is transformed to moving coordinates and Laplace transform is used to develop the exact solution of this problem in quasi-steady state. Twelve cases have been studied that cover constant temperature and flux conditions imposed on the moving front. The interface positions and the temperatures in the medium can be derived in closed forms for eight cases. For the four cases whose solutions cannot be derived in a closed form, procedures for exact solution of the problems are given in great detail. Numerical examples are also provided for a parametric study of the problems.

INTRODUCTION

Stefan problems that can be solved exactly must be adaptable to a similarity transformation. This restricts the problems to be solved in an unbounded medium which is made of a material of constant thermophysical properties and is imposed with a constant temperature boundary condition [1, 2]. With the severe limitation imposed by the exact solution, there have been numerous efforts documented in the literature devoted to the development of approximate solutions that encompass use of power series expansions [3, 4], polynomial expansions in terms of complimentary error functions [5], solutions by means of integrodifferential equations [6, 7], coordinate transformations [8, 9], asymptotic expansions based on perturbation techniques [10, 11], complex variables [12, 13], source-and-sink methods [14, 15], heat balance integrals [16, 17], and even inverse solution techniques [18, 19]. Following a different approach, the problems have been solved by using a weak formulation in terms of enthalpy [20, 21] and in terms of specific heat [22], and the variational formulation [23, 24]. Numerical techniques have also been developed, which include use of a boundary element method [25, 26] and an incremental linearization scheme based on the source-and-sink method [27–29].

It is the intention of this paper to present an exact solution that does not require use of the similarity transformation. It is concerned with the phase change in an infinite medium heated by a plane heat front moving at a constant velocity in a fixed direction. The medium has equal phase properties and may or may not dissipate heat to the surroundings. Specifically, the exact solutions will be developed when the heat transfer in the medium has reached a quasi-steady state, a point in time when the initial transient period is over.

The problem analyzed in this paper is somewhat similar to the classical one-dimensional moving-heat-front problems studied by Rosenthal [30]. However, no phase change has been considered in his work. The moving heat front problem is important because of recent interest in welding and annealing in which the heat transfer in the medium is usually solved by a numerical method (e.g. Grigoropoulos and Dutcher [31]). The analysis given in this paper thus serves three purposes. It demonstrates that the exact solutions can be obtained for a Stefan problem imposed with a moving heat front in a quasi-steady state. It also complements Rosenthal's work on moving heat front studies by inclusion of a phase change. Finally, it provides limiting cases by which the numerical methods developed for the solution of the welding and annealing problems can be checked for accuracy.

ANALYSIS

The problem at hand can be formulated by means of a source-and-sink method in the fixed coordinate x. The equations will be given with the variables expressed in primitive forms first for the sake of clarity [27, 28].

Governing equation:

$$\frac{\partial^2 T}{\partial x^2} - m^2 T - \frac{\rho L}{k}\frac{\mathrm{d}x}{\mathrm{d}t}\delta(x-R_i) = \frac{1}{\alpha}\frac{\partial T}{\partial t},$$

$$T(x,t) \quad \begin{matrix} -\infty < x < \infty \\ t > 0 \end{matrix} \quad i = a, b. \qquad (1)$$

Initial condition:

NOMENCLATURE

a, b	equation (9a)
c	equation (9b), specific heat
d	equation (9b)
k	thermal conductivity
L	latent heat for melting or freezing
M	equation (13a)
m	heat dissipation coefficient
N	equation (13b)
q	heat flux
R	interface position
St	Stefan number
s	equation (9c)
T	temperature
t	time
V	velocity of moving heat front
x	position in fixed coordinate.

Greek symbols

α	thermal diffusivity
δ	Dirac-delta function
ζ	dimensionless position
η	moving coordinate pointed opposite to ξ
θ	dimensionless temperature
ξ	moving coordinate
ρ	dimensionless interface position, density
ω	dimensionless heat flux.

Subscripts

a, b	interface positions in fixed coordinate
i	dummy representing either a or b
m	melting temperature
o	temperature at the moving heat front
oa, ob	interface positions in moving coordinate
p	constant pressure condition
q	the moving heat front under specified flux condition
T	the moving heat front under specified temperature condition
th	threshold
ub	upper bound.

$$T(x,0) = 0 < T_{\mathrm{m}}. \tag{2}$$

Boundary conditions:

$$T(Vt,t) = T_{\mathrm{o}}$$

or

$$-k\left[\frac{\partial T(Vt^{+},t)}{\partial x} - \frac{\partial T(Vt^{-},t)}{\partial x}\right] = q^{+}+q^{-} = q \tag{3a, b}$$

$$T(-\infty,t) = \text{finite} \tag{3c}$$

$$T(\infty,t) = 0. \tag{3d}$$

Interface conditions:

$$T(R_i,t) = T_{\mathrm{m}}, \quad i = \mathrm{a}, \mathrm{b}. \tag{4a, b}$$

Here the Dirac-delta term in equation (1) vanishes if the heat flux, q, released by the moving heat front is small, so that it is insufficient to cause phase change. If the heat flux is large, phase change takes place. Then, the temperature in the medium is divided into two branches: $-\infty < x < Vt$ and $Vt < x < \infty$. In the branch behind the front ($-\infty < x < Vt$), the Dirac-delta term models a source front that locates the interface position in this branch, whereas in the branch ahead of the front ($Vt < x < \infty$), the Dirac-delta term models a sink front that locates the interface position in that branch. The interface ahead of the moving heat front is designated R_{a}, while that behind the front is designated R_{b}. In the fixed coordinate, these interfaces are moving together with the imposed heat front in the positive x-direction.

Equations (3a) and (3b) provide a constant temperature or a constant heat flux condition that may be imposed at the moving front, where x is equal to Vt product. Notice that the interface Stefan conditions have been incorporated into equation (1), which can be readily verified by integrating equation (1) across the interface in question [29]. Equations (4a) and (4b) give the temperature condition at the interfaces.

For the solution of the problem in quasi-steady state in the range of $Vt < x < \infty$, one introduces a transformation that relates ξ and x as $\xi = x - Vt$, as suggested by Rosenthal [30]. On the other hand, for the solution of the problem in the quasi-steady state in the range of $-\infty < x < Vt$, one introduces a different transformation that relates η and x as $\eta = Vt - x$ (see Fig. 1). Then, the quasi-steady problems in two branches are all expressed in the same range of 0–∞. The problems can be formulated as follows.

Governing equations:

$$\begin{matrix} \mathrm{d}^2T/\mathrm{d}\xi^2 \\ \mathrm{d}^2T/\mathrm{d}\eta^2 \end{matrix} + \left(\frac{V}{\alpha}\right)\begin{matrix} \mathrm{d}T/\mathrm{d}\xi \\ \mathrm{d}T/\mathrm{d}\eta \end{matrix} - m^2T = \left(\frac{\rho VL}{k}\right)$$

$$\begin{matrix} \delta(\xi - R_{\mathrm{oa}}) & T(\xi) & 0 < \xi < \infty \\ \delta(-\eta + R_{\mathrm{ob}}) & T(\eta) & 0 < \eta < \infty \end{matrix}. \tag{5a, b}$$

Boundary conditions:

$$T(0) = T_{\mathrm{o}} \quad (\text{if } T_{\mathrm{o}} \text{ is given}) \tag{6a}$$

$$\frac{\mathrm{d}T(0)}{\mathrm{d}\xi} = -\frac{q^{+}}{k} \quad \frac{\mathrm{d}T(0)}{\mathrm{d}\eta} = -\frac{q^{-}}{k}$$

$$q = q^{+}+q^{-} \quad (\text{if } q \text{ is given}) \tag{6b–d}$$

$$T(\xi = \infty) = 0 \tag{6e}$$

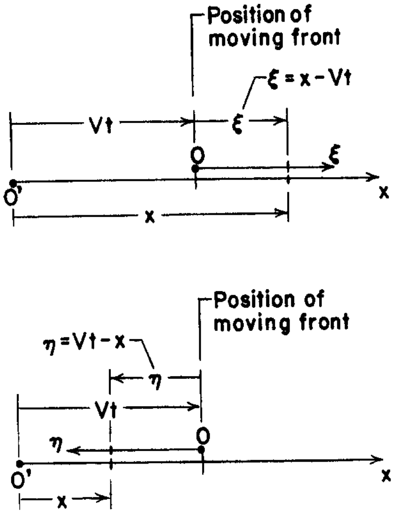

Fig. 1. Change from fixed to moving coordinates.

$$T(\eta = \infty) = \text{finite}. \tag{6f}$$

Interface conditions:

$$T(R_{oi}) = T_m \quad i = \text{a, b}. \tag{7a, b}$$

In the formulation above, the phase change problems have been expressed in moving coordinates in the search for quasi-steady solutions. Notice that, in moving coordinates, R_{oa} and R_{ob} are used to represent the interface positions.

Equations (5a, b) share the same range of ξ and η; they can be solved by a Laplace transform [32]. In this effort, the Dirac-delta functions are expanded in terms of Heaviside functions and the Laplace transform is applied to these functions. The shifting theorem in the transform is then used to recover the temperatures for the delta term in the ξ and η axes. Finally, for that solution of T in $0 < \eta < \infty$, a reversal of the η axis, which calls for changing η to $-\xi$, R_{ob} to $-R_{ob}$ and $dT(0)/d\eta$ to $-dT(0)/d\xi$, transforms the temperature in this branch in terms of ξ. The quasi-steady solution results can be summarized as follows:

$$T(\xi) = \left[T'(0^-) + \frac{V}{\alpha}T(0)\right]\frac{e^{-c\xi} - e^{-d\xi}}{d-c} + T(0)\frac{ce^{-c\xi} - de^{-d\xi}}{c-d} + \frac{\rho VL}{k}\frac{e^{-c(\xi - R_{ob})} - e^{-d(\xi - R_{ob})}}{c-d}$$

$$\text{for } \xi < R_{ob} \tag{8a}$$

$$T(\xi) = \left[T'(0^-) + \frac{V}{\alpha}T(0)\right]\frac{e^{-c\xi} - e^{-d\xi}}{d-c} + T(0)\frac{ce^{-c\xi} - de^{-d\xi}}{c-d}$$

$$\text{for } R_{ob} < \xi < 0 \tag{8b}$$

$$T(\xi) = \left[T'(0^+) + \frac{V}{\alpha}T(0)\right]\frac{e^{a\xi} - e^{b\xi}}{a-b} + T(0)\frac{ae^{a\xi} - be^{b\xi}}{a-b}$$

$$\text{for } 0 < \xi < R_{oa} \tag{8c}$$

$$T(\xi) = \left[T'(0^+) + \frac{V}{\alpha}T(0)\right]\frac{e^{a\xi} - e^{b\xi}}{a-b} + T(0)\frac{ae^{a\xi} - be^{b\xi}}{a-b} + \frac{\rho VL}{k}\frac{e^{a(\xi - R_{oa})} - e^{b(\xi - R_{oa})}}{a-b}$$

$$\text{for } \xi > R_{oa} \tag{8d}$$

where

$$\begin{matrix} a \\ b \end{matrix} = \pm\frac{V}{2\alpha}(s \mp 1) \gtrless 0 \quad \begin{matrix} c \\ d \end{matrix} = \pm\frac{V}{2\alpha}(s \pm 1) \gtrless 0$$

$$s = \left[1 + \left(\frac{2m\alpha}{V}\right)^2\right]^{1/2}. \tag{9a–c}$$

Equations (8a)–(8d) are general and can be applied to both types of conditions imposed at the moving heat front. In this effort, they must satisfy conditions (6e) and (6f). It follows that

$$T'(0^+) + \left(\frac{V}{\alpha} + a\right)T(0) + \frac{\rho VL}{k}e^{-aR_{oa}} = 0 \tag{10a}$$

and

$$T'(0^-) + \left(\frac{V}{\alpha} - c\right)T(0) - \frac{\rho VL}{k}e^{-cR_{ob}} = 0. \tag{10b}$$

These equations can be used to simplify (8a)–(8d).

Class A problem—imposed temperature at the heat front

For a constant temperature imposed at the moving heat front [equation (3a)], it is convenient to express the medium temperature in four branches as

$$\theta(\zeta < \rho_{ob}) = \left[\theta_o - \frac{1}{Sts}(N^d - N^c)\right]e^{-d(\alpha/V)\zeta} \tag{11a}$$

$$\theta(\rho_{ob} < \zeta < 0) = \left[\theta_o + \frac{1}{Sts}N^c(1 - e^{-s\zeta})\right]e^{-d(\alpha/V)\zeta} \tag{11b}$$

$$\theta(0 < \zeta < \rho_{oa}) = \left[\theta_o + \frac{1}{Sts}M^a(1 - e^{s\zeta})\right]e^{b(\alpha/V)\zeta} \tag{11c}$$

$$\theta(\zeta > \rho_{oa}) = \left[\theta_o - \frac{1}{Sts}(M^b - M^a)\right]e^{b(\alpha/V)\zeta}. \tag{11d}$$

Here, for the sake of generality, the equations are cast in dimensionless forms defined as

$$\frac{T}{T_m} = \theta \quad \frac{\xi}{(\alpha/V)} = \zeta \quad \frac{c_p T_m}{L} = St \quad \frac{T_o}{T_m} = \theta_o$$

$$\frac{q}{\rho VL} = \omega \quad \frac{R_{oi}}{(\alpha/V)} = \rho_{oi} \quad i = \text{a, b}. \tag{12a–g}$$

Notice that, in equations (11a)–(11d), the interface positions ρ_{oa} and ρ_{ob} have been expressed in terms of M and N as

$$\rho_{oa} = -\frac{V}{\alpha}\ln M \tag{13a}$$

$$\rho_{ob} = \frac{V}{\alpha}\ln N. \tag{13b}$$

These M and N become the new unknowns to be determined.

To find the interface positions for this class of problems, one sets ξ and T in equation (11c) to R_{oa} and T_m, respectively. This gives

$$\theta_o M^{-b} - \frac{1}{Sts}(1 - M^{sV/\alpha}) - 1 = 0. \tag{14}$$

Likewise, setting ξ and T in equation (11b) to R_{ob} and T_m, respectively, gives

$$\theta_o N^{-d} - \frac{1}{Sts}(1 - N^{sV/\alpha}) - 1 = 0. \tag{15}$$

These equations can be solved individually for M and N.

To find the heat flux at the moving heat front, one introduces equations (10a) and (10b) into equations (6b)–(6d), in which η in equation (6c) is changed to $-\xi$. It follows that

$$\omega = Sts\theta_o + M^a + N^c. \tag{16}$$

The ratio of heat that transfers forward to that transfers backward can be derived as

$$(RATIO)_T = -\frac{St(1+s)\theta_o + e^{-(s-1)\rho_{oa}/2}}{St(1-s)\theta_o - e^{-(s+1)\rho_{ob}/2}}. \tag{17}$$

This completes the solution of the problem for a temperature condition imposed on the heat front.

Class B problem—imposed flux at the heat front

For a constant heat flux imposed at the moving heat front [equation (3b)], $q+$, $q-$, and $T(0)$ are all unknown. It is convenient to derive the temperature equations in the following forms:

$$\theta(\zeta < \rho_{ob}) = \frac{1}{Sts}(\omega - M^a - N^d)e^{-d(\alpha/V)\zeta} \tag{18a}$$

$$\theta(\rho_{ob} < \zeta < 0) = \frac{1}{Sts}(\omega - N^c e^{-s\zeta} - M^a)e^{-d(\alpha/V)\zeta} \tag{18b}$$

$$\theta(0 < \zeta < \rho_{oa}) = \frac{1}{Sts}(\omega - M^a e^{s\zeta} + N^c)e^{b(\alpha/V)\zeta} \tag{18c}$$

$$\theta(\zeta > \rho_{oa}) = \frac{1}{Sts}(\omega - M^b + N^c)e^{b(\alpha/V)\zeta}. \tag{18d}$$

To derive equations to solve for M and N, equations (14)–(16) are combined to give

$$(Sts+1)M^b + \left(\frac{\omega - M^a}{Sts+1}\right)^{c/d} - \omega = 0 \tag{19}$$

and

$$N = \left(\frac{\omega - M^a}{Sts+1}\right)^{1/d}. \tag{20}$$

In this case, equation (19) will be used first to solve for M, which is, in turn, used in equation (20) to solve for N. Once they are found, they can again be used in equation (16) to find $T(0)$. The ratio of heat that transfers forward to backward can also be derived as

$$(RATIO)_q = -\frac{(1+s)(\omega - e^{(s+1)\rho_{ob}/2}) - e^{-(s-1)\rho_{oa}/2}}{(1-s)(\omega - e^{-(s-1)\rho_{oa}/2}) - e^{(s+1)\rho_{ob}/2}}. \tag{21}$$

The problem is then solved completely.

SPECIALIZATION

The analysis developed above is general, which can be used to solve 12 different cases summarized in Tables 1 and 2. Six cases are solved for the Class A problem (imposed temperature at the heat front) as listed in Table 1. In this table, the simplest cases (a and b) are the ones for a heat front that releases only a small amount of heat so that no phase change takes place. Here, case a is for the medium without heat loss to the surroundings ($m = 0$), while case b is for the medium with heat loss to the surroundings ($m > 0$). Results tabulated for these cases can be easily derived by using the equations given in this paper in which terms containing $\rho VL/k$ in equations (8a)–(8d) are discarded for heat transfer without phase change. This is equivalent to setting M and N to zero in the dimensionless equations. Notice that the temperature derived for case a for $\zeta > 0$ corresponds to that problem of melting with continuous removal of the melt as analyzed by Landau [33].

Cases c and d refer to a situation when the heat released by the front is large enough to cause phase change. Both are for the medium without heat loss to the surroundings; m is thus taken to be zero. Case c is for the medium initially at the phase change temperature ($T_m = 0$), while case d is for the medium with the phase change temperature that is higher than the initial temperature ($T_m > 0$). The former thus represents a one-phase problem, while the latter represents a two-phase problem. Expectedly, ρ_{ob} is located at $-\infty$ for both cases and, consequently, N is zero. The other interface position, ρ_{oa}, can be found by using equation (14). Closed-form expressions can be derived for this position as well as the temperatures for cases c and d, as listed in the table. It is noted that, for a constant temperature imposed on the heat front, the results are quite similar for the one- and two-phase problems. For example, the temperatures behind the front are identical. Even the temperature equations in

Table 1. Summary of equations for Class A problems

Case	m	L	T_m	$\theta(\zeta < \rho_{ob})$	$\theta(\rho_{ob} < \zeta < 0)$	$\omega(\zeta = 0)$	$\theta(0 < \zeta < \rho_{oa})$	$\theta(\zeta > \rho_{oa})$	ρ_{oa}	ρ_{ob}
a	0	0	—	θ_o		$St\theta_o$	$\theta_o e^{-\zeta}$		—	—
b	>0	0	—	$\theta_o e^{(s-1)\zeta/2}$		$Sts\theta_o$	$\theta_o e^{-(s+1)\zeta/2}$		—	—
c	0	>0	0	θ_o		$1+St\theta_o$	$\left[\theta_o + \frac{1}{St}(1-e^{\zeta})\right]e^{-\zeta}$	0	$\ln(1+St\theta_o)$	—
d	0	>0	>0	θ_o		$1+St\theta_o$	$\left[\theta_o + \frac{1}{St}(1-e^{\zeta})\right]e^{-\zeta}$	$\left(\theta_o + \frac{1-\theta_o}{1+St}\right)e^{-\zeta}$	$\ln\left(\frac{1+St\theta_o}{1+St}\right)$	—
e	>0	>0	0	(11a)	(11b)	(16)	(11c)	(11d)	(14)	(15)
f	>0	>0	>0	(11a)	(11b)	(16)	(11c)	(11d)	(14)	(15)

Table 2. Summary of equations for Class B problems

Case	m	L	T_m	$\theta(\zeta < \rho_{ob})$	$\theta(\rho_{ob} < \zeta < 0)$	$\theta(\zeta = 0)$	$\theta(0 < \zeta < \rho_{oa})$	$\theta(\zeta > \rho_{oa})$	ρ_{oa}	ρ_{ob}
a	0	0	—	$\frac{\omega}{St}$		$\frac{\omega}{St}$	$\frac{\omega}{St}e^{-\zeta}$		—	—
b	>0	0	—	$\frac{\omega}{Sts}e^{(s-1)\zeta/2}$		$\frac{\omega}{Sts}$	$\frac{\omega}{Sts}e^{-(s+1)\zeta/2}$		—	—
c	0	>0	0	$\frac{\omega}{St}\left(1-\frac{1}{\omega}\right)$		$\frac{\omega}{St}\left(1-\frac{1}{\omega}\right)$	$\frac{\omega}{St}\left(e^{-\zeta}-\frac{1}{\omega}\right)$	0	$\ln\omega$	—
d	0	>0	>0	$\frac{\omega}{St}\left(1-\frac{1}{\omega}\right)$		$\frac{\omega}{St}\left(1-\frac{1}{\omega}\right)$	$\frac{\omega}{St}\left(e^{-\zeta}-\frac{1}{\omega}\right)$	$\frac{\omega}{St}\frac{St}{1+St}e^{-\zeta}$	$\ln\left(\frac{\omega}{1+St}\right)$	—
e	>0	>0	0	(18a)	(18b)	(16)	(18c)	(18d)	(19)	(20)
f	>0	>0	>0	(18a)	(18b)	(16)	(18c)	(18d)	(19)	(20)

the range of $0 < \zeta < \rho_{oa}$ are identical for the two cases. However, this should not be taken as their having the same profiles, because their interface positions are different.

Similar cases are analyzed in Table 2 for the Class B problem (imposed flux at the heat front). It is expected that, for this class, the results for cases a and b can be recast so that they conform to the expressions derived by Rosenthal [30] for heat diffusion without phase change. As for case c, N is again zero. This permits the front interface position, ρ_{oa}, to be found directly from equation (20). It is noted that, for this case, because ρ_{oa} is equal to $\ln \omega$, the temperature behind the heat front is independent of the interface position. Similar results can be obtained for case d as listed in the table.

RESULTS AND DISCUSSION FOR CASES e AND f

Physically, in each table, cases c and d provide upper bound for ρ_{oa} for cases e and f, respectively. Furthermore, case e can be considered a special case of case f. Then, if the heat front is imposed with a temperature condition, the upper bound for ρ_{oa} can be established in a general form as

$$\rho_{oa,ub,T} = \ln\left(\frac{1+St\theta_o}{1+St}\right). \tag{22}$$

Correspondingly, the upper bound for ρ_{ob} can be established as

$$\rho_{ob,ub,T} = -\ln\left(\frac{1+St\theta_o}{1+St}\right). \tag{23}$$

A close examination of equations (14) and (15) reveals some characteristics which are important to the numerical solution of the interface positions with these equations. It can be shown that the left hand side of equation (14) has a value that decreases monotonically with the increase of ρ_{oa}. On the other hand, the left hand side of equation (15) increases monotonically with the increase of ρ_{ob}. Since both of these sides have a value $(\theta_o - 1) > 0$ at ρ_{oa} and ρ_{ob} equal to zero, the interface positions can always be found uniquely when a temperature condition is imposed on the front.

As for the case of a flux condition imposed on the front, the temperature at the front becomes an unknown. It is necessary to check if the imposed heat flux is of a value higher than the threshold for phase change. This threshold flux can be derived by setting M and θ_o in equations (16) and (20) to unity and combining these equations. The threshold flux can then be solved as

$$\omega_{th} = Sts + 2. \tag{24}$$

The upper bound for ρ_{oa} can be established as

$$\rho_{oa,ub,q} = \ln\left(\frac{\omega}{1+St}\right). \tag{25}$$

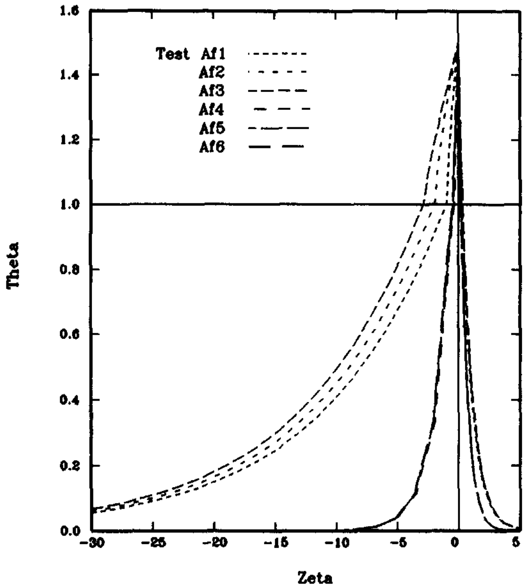

Fig. 2. A parametric study of Stefan problems of case f in Class A.

Notice that, when a heat flux condition is imposed on the front, the left hand side of equation (19) has a value $(\omega_{th} - \omega) < 0$ at ρ_{oa} equal to zero. This side increases monotonically with ρ_{oa}. Hence, a unique solution of ρ_{oa} is assured as long as $\omega > \omega_{th}$. Also for this case, the interface position behind the front, ρ_{ob}, can be found directly by using equation (20); no iteration is thus necessary. The nonlinear equations given in this paper can be solved accurately by means of a bisection method or the Newton–Raphson method.

Equations given in this paper have been used to run tests for case f in Tables 1 and 2. The results are plotted in Figs. 2 and 3. In Fig. 2, the moving heat front is imposed with a constant temperature. All the parameters tested in this figure have been summarized in Table 3, where the results are also tabulated for the temperature and the heat flux at the moving front, the interface positions, and the ratio of heat transfer. As expected, the designation Af1 (first column) refers to test 1 in Class A and case f. Six tests have thus been made in this figure. It is noted that, for all the numerical results presented in this paper, the interface positions were solved by using a bisection method which was converged to 10^{-6}.

In all the tests performed in Fig. 2, the temperature profiles ahead of the front behave quite similarly—all are very steep, which makes it difficult to visually detect the temperature-slope discontinuity at interface in this region. However, the temperature profiles behind the front deviate noticeably to the extent that their behaviors can be easily visualized. Take Af1–Af3 behind the front for example. The curves spread out evenly, a result of the change of the Stefan number, a ratio of the sensible heat to the latent heat. A heat front moving in a medium of large Stefan number (or small latent heat) thus has an effect of

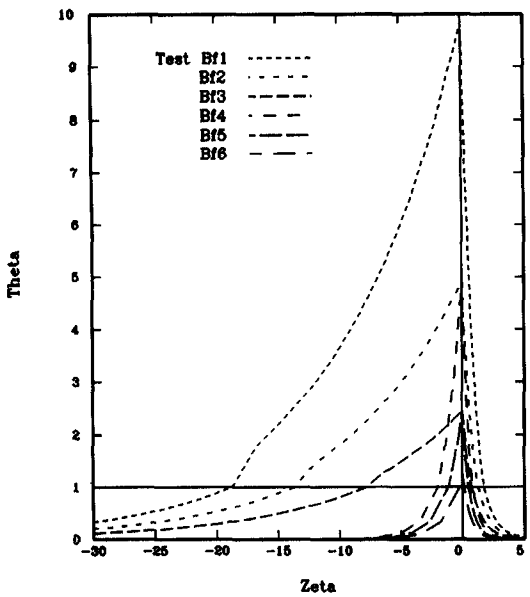

Fig. 3. A parametric study of Stefan problems of case f in Class B.

leaving behind a large melted pool, a fact which is physically justified. On the other hand, a doubling of the parameter s tends to reduce the size of this melted pool (see tests Af4–Af6). This can certainly be attributed to the large $m\alpha/V$ ratio as defined for this parameter in equation (9c). It is also noted that, when the s value is increased, the medium temperature behind the front becomes less dependent on the Stefan number as the curves fall one on top of the other. For all the cases tested, the magnitude of ρ_{ob} is always greater than ρ_{oa}, a result of the motion of the front. Of particular interest in this figure is the difference in the temperature curvature across the interface behind the moving front. In the liquid region, the curves have a slight curvature bent downward, whereas in the solid region, the curves bent upward. This trend persists in the study of Class B problems in the paragraphs that follow.

Six tests have been performed for Class B, case f. As shown in Fig. 3, when the flux condition is imposed at the moving front, the temperature at the front moves up and down along the zero axis in response to the imposed flux. The temperature curves thus spread out, which facilitates viewing their trends in the figure. Attention is first directed to those curves located ahead of the front. Here, the curves exhibit a different behavior under the imposed flux condition. For example, an increase of the Stefan number under the same flux condition (see tests Bf1–Bf3 listed in Table 3) is able to relocate the interface positions so that the curve with the largest Stefan number has the smallest value of ρ_{oa}. This can be alluded to the rapid drop of the dimensionless front temperature for this curve, as shown in Fig. 3. Nevertheless, it reverses the trend found earlier for the front imposed with a constant temperature condition (refer to ρ_{oa} data for tests Af1–Af3 in Table 3). It should be noted that the trends observed here are also related to how the dimensionless groups are defined, a fact well known in the explanation of heat transfer phenomena.

The same trend is found for those curves located behind the front. Here, in further reinforcement of what was discovered earlier for the front imposed with a constant temperature condition, the temperature behind the front exhibits the same curvature variations across the interface. As a result, for the case of large heat flux (Bf1), there is a distinct inflection point for the temperature curve in the liquid region. This is believed to be the combination of the effects of the heat dissipation in conjunction with medium refreezing. This trend is not found in conventional Stefan problems.

It is also interesting to compare the heat transfer ratio for the two classes of problems. As shown in Table 3, when a flux condition is imposed on the front, this ratio is found to be insensitive to the change of the Stefan number. Yet, it is highly sensitive to the change of s. Such trends, however, are not found in the case of the imposed temperature. For example, in tests Af1–Af3 where the s value is low, the heat transfer ratio increases with the Stefan number. Yet, it is able to hold steady at about 2.4 for the case of large s value, as shown for tests Af4–Af6 in the table. Notice that, for a flux condition imposed on the front, the

Table 3. Compilation of data for a parametric study of case f in Classes A and B

Test	St	s	θ_o	ω	ρ_{oa}	ρ_{ob}	Ratio
Af1	1.625	1.2	1.5	4.234	0.2538	−0.9966	7.713
Af2	3.25	1.2	1.5	6.935	0.3006	−1.967	10.73
Af3	6.5	1.2	1.5	12.71	0.3312	−2.884	11.25
Af4	1.625	2.4	1.5	7.255	0.1865	−0.3764	2.326
Af5	3.25	2.4	1.5	13.02	0.2094	−0.4616	2.395
Af6	6.5	2.4	1.5	24.67	0.2231	−0.5157	2.418
Bf1	1.625	1.2	9.825	20	1.740	−18.71	11.26
Bf2	3.25	1.2	4.903	20	1.279	−13.62	11.28
Bf3	6.5	1.2	2.445	20	0.7463	−7.735	11.29
Bf4	1.625	2.4	4.975	20	0.8263	−1.969	2.47
Bf5	3.25	2.4	2.453	20	0.4785	−1.121	2.46
Bf6	6.5	2.4	1.176	20	0.0882	−0.1974	2.36

threshold heat flux must be evaluated prior to the formal solution of the problem. Of those tested in Table 3, Bf6 has the largest threshold flux (17.6). This leads to the smallest θ_o value (1.176) in the group. The temperature at the moving front is found to rise slowly beyond the melting point, a fact which makes the evaluation of the threshold flux an important procedure in the solution of the Stefan problems.

CONCLUDING REMARKS

The equations derived in this paper have been tested rigorously for accuracy. This is necessary since exact solutions have not been available for the classes of the problems studied here, while numerical solutions of the Stefan problems themselves are, after all, inexact, which make them inadequate for comparison. In this effort, use was made of case f for tests because of its generality, and the test for exactness was made by substituting equations (11) and (18) into equations (1), (3), and (4). Additionally, temperatures have also been tested for continuity at the heat front and the interface positions. These temperature equations have also been tested for their satisfaction of the Stefan conditions generated by using equation (1). In all tests, the original governing equation and boundary conditions are satisfied exactly.

The source-and-sink method has shown to be attractive in the solution of the Stefan problems given in this paper. Using one set of equations to solve temperatures in four regions, the source-and-sink method is ideally suited to the solution of the present problems by Laplace transform. In this method, the general solutions are expressed in terms of the temperature and its slopes at both sides of the moving front. The boundary conditions can thus be applied readily to complete the solution. The source-and-sink method given in this paper provides an effective approach for an exact solution of the Stefan problems.

REFERENCES

1. L. S. Yao and J. Prusa, Melting and freezing, *Adv. Heat Transfer* **19**, 1–95 (1989).
2. J. Crank, *Free and Moving Boundary Problems*. Clarendon Press, London (1984).
3. G. W. Evans, E. Isaacson and J. K. L. MacDonald, Stefan-like problems, *Q. Appl. Math.* **8**, 312–319 (1950).
4. S. H. Cho and J. E. Sunderland, Approximate temperature distribution for phase change of a semi-infinite body, *J. Heat Transfer* **103**, 401–403 (1981).
5. L. N. Tao, On free boundary problems with arbitrary initial and flux conditions, *J. Appl. Math. Phys.* **30**, 416–426 (1979).
6. N. M. H. Lightfoot, Solidification of molten steel, *Proc. Lond. Math. Soc.* **31**, 97–116 (1929).
7. B. A. Boley, The embedding technique in melting and solidification problems, *Moving Boundary Problems in Heat Flow and Diffusion, Proceedings of a Conference*, University of Oxford, 25–27 March, pp. 150–172 (1974).
8. J. L. Duda, M. F. Malone, R. H. Notter and J. S. Vrentas, Analysis of two-dimensional diffusion-controlled moving boundary problems, *Int. J. Heat Mass Transfer* **18**, 901–910 (1975).
9. T. Saitoh, Numerical method for multidimensional freezing problems in arbitrary domains, *J. Heat Transfer* **100**, 294–299 (1978).
10. S. Weinbaum and L. M. Jiji, Singular perturbation theory for melting or freezing in finite domains not at the fusion temperature, *J. Appl. Mech.* **44**, 25–30 (1977).
11. Ch. Charach and P. Zolgin, Solidification in a finite initially overheated slab, *Int. J. Heat Mass Transfer* **28**, 2261–2268 (1985).
12. R. Siegel, Cauchy method for solidification interface shape during continuous casting, *J. Heat Transfer* **105**, 667–671 (1983).
13. J. G. Nyros and C. K. Hsieh, Combination of source-and-sink method and complex-temperature method for the solution of Stefan problems imposed with cyclic temperature and flux conditions, *J. Heat Transfer*, in press.
14. H. Li, C. K. Hsieh and D. Y. Goswami, Source-and-sink method of solution of two dimensional phase change for energy storage, *J. Solar Energy Engng* **116**, 100–106 (1994).
15. M. Akbari and C. K. Hsieh, Solution of ablation and combination of ablation and Stefan problems by a source-and-sink method, *Numer. Heat Transfer, Part A* **26**, 67–86 (1994).
16. T. R. Goodman, Application of integral methods to transient nonlinear heat transfer, *Adv. Heat Transfer* **1**, 71–79 (1964).
17. J. Mennig and M. N. Ozisik, Coupled integral equation approach for solving melting or solidification, *Int. J. Heat Mass Transfer* **28**, 1481–1485 (1985).
18. N. Zabaras, S. Mukherjee and O. Richmond, An analysis of inverse heat transfer problems with phase changes using an integral method, *J. Heat Transfer* **110**, 554–560 (1988).
19. C. K. Hsieh, M. Akbari and H. Li, Solution of inverse Stefan problems by a source-and-sink method, *Int. J. Numer. Meth. Heat Fluid Flow* **2**, 391–406 (1992).
20. C. M. Elliot and J. R. Ockendon, Weak and variational methods for moving boundary problems. In *Research Notes in Mathematics* 59. Pitman, Boston (1982).
21. V. Voller and M. Cross, Accurate solutions of moving boundary problems using the enthalpy method, *Int. J. Heat Mass Transfer* **24**, 545 (1981).
22. L. E. Goodrich, Efficient numerical technique for one-dimensional thermal problems with phase change, *Int. J. Heat Mass Transfer* **21**, 615 (1978).
23. T. J. Lardner, Approximate solutions to phase-change problems, *AIAA J.* **5**, 2079–2080 (1967).
24. N. Prasad, Melting of solid bodies due to convective heating with the removal of melt, *J. Spacecraft* **16**, 445–448 (1979).
25. K. O'Neill, Boundary integral equation solution for moving boundary phase change problems, *Int. J. Numer. Meth. Engng* **19**, 1825–1850 (1983).
26. C. K. Hsieh, Unification of source-and-sink method and boundary element method for the solution of potential problems, *J. Heat Transfer* **115**, 775–777 (1993).
27. C. Y. Choi and C. K. Hsieh, Solution of Stefan problems imposed with cyclic temperature and flux boundary conditions, *Int. J. Heat Mass Transfer* **35**, 1181–1195 (1992).
28. C. K. Hsieh and C. Y. Choi, Solution of one- and two-phase melting and solidification problems imposed with constant or time-variant temperature and flux boundary conditions, *J. Heat Transfer* **114**, 524–528 (1992).
29. C. K. Hsieh and C. Y. Choi, A general analysis of phase-change energy storage for solar energy applications, *J. Solar Energy Engng* **114**, 203–211 (1992).
30. D. Rosenthal, The theory of moving sources of heat and

its application to metal treatments, *Trans. ASME* **68**, 849–866 (1946).
31. C. P. Grigoropoulos and W. E. Dutcher, Jr, Moving front fixing in thin film laser annealing, *J. Heat Transfer* **114**, 271–277 (1992).
32. P. M. Morse and H. Feshbach, *Methods of Theoretical Physics*. McGraw-Hill, New York (1953).
33. H. G. Landau, Heat conduction in a melting solid, *Q. Appl. Math.* **8**, 81–94 (1950).